# Non-spherical dark matter structures detection

# Nicolas Loizeau and Glennys R. Farrar

Center for Cosmology and Particle Physics, Department of Physics, New York University, 726 Broadway, New York, NY, U.S.A.

E-mail: nicolas.loizeau@nyu.edu, glennys.farrar@nyu.edu

Received November 22, 2021 Revised February 21, 2022 Accepted February 27, 2022 Published March 21, 2022

**Abstract.** A rotation curve inequality that holds for spherically symmetric mass distributions is derived, and tested against the SPARC galaxy rotation curves dataset. We identify several Galaxies, e.g. NGC7793 and UGC11557, which are candidates for hosting non-spherical dark matter structures that could be detected by more precise measurements.

**Keywords:** galaxy dynamics, rotation curves of galaxies

**ArXiv ePrint:** 2106.14915

1	Introduction	1
2	Spherical inequalities	2
3	Examples	3
4	Asphericity of the DM distribution in the SPARC galaxies	3
5	Conclusion	7

#### 1 Introduction

Contents

Cosmological simulations predict that the dark matter halos of low-redshift galaxies are triaxial on large scales. In addition to such very large scale asphericity, an interaction between dark matter and baryons could lead to an accumulation of dark matter in regions of gas overdensities, resulting in a (puffy) DM disk or other structure in the inner galaxy. Here we propose a strategy for detecting such small-scale DM structures if they exist.

Energy transfer is most efficient in collisions between similar mass particles, so a DM accumulation in the vicinity of baryons would be greatest for DM whose mass is of order the mass of H and He, and likely undetectably small for significantly lower and higher mass DM. The random velocities of DM particles in the halo are generally larger than those of gas in the disk, so on average a DM-baryon collision causes the DM particle final phase space to approach that of the initial baryon. The scattering heats the gas, which then re-cools through standard mechanisms. (An almost infinitesimal fraction of DM particles intersect a star; those would just reflect or more usually be trapped in the star, negligibly impacting the global DM distribution.) The net DM accumulation would be greatest around the longest-lived gas structures and of course would be proportional to the cross-section between DM and baryons.

Our purpose here is to introduce a practical and unambiguous diagnostic of structure in the distribution of DM on small scales, as could result from DM-baryon interactions.

Rotation curves are central tools to study the mass distribution of individual galaxies [1]. The dark matter distribution can be estimated by subtracting the baryonic components from the observed mass distribution. There is a degeneracy in the mass distribution determination using rotation curves: two different mass distributions can lead to the same rotation curve. This degeneracy can be broken by imposing that the DM distribution have a particular functional form. Common DM halo models are spherically symmetric. A given DM distribution model can be favored/excluded because it gives better/worse rotation curves fits, but being able to rigorously exclude a model based on incompatibilities with some rotation curve features would be a powerful tool. One feature to consider is sphericity. Whether DM disks, or DM structures such as non-monotonic radial density exist, is still an open question [2–5].

In a previous paper, we fit 121 galaxy rotation curves with a hadronically interacting dark matter (HIDM) model composed of a DM halo and a DM disk that scales the halo-baryons interactions [6]. We showed that this model outperforms 7 other canonical DM and

modified gravity models. This finding motivates the need for having other, model independent, indicators of non-spherical dark mater structures in galaxies. (Note that the analysis does not reveal the thickness of the DM disk, which is presumably thick.)

Some non-spherical mass distributions can produce rotation curves that are impossible to build from a spherical distribution. For example, a ring of mass produces an outward gravitational pull inside of the ring, a phenomena that is impossible to reproduce with a spherical mass distribution. We propose a method to detect some such asphericities and test it on the SPARC rotation curves dataset [7].

In sections 2 and 3 we derive a general asphericity diagnostic for rotation curves and test it on some ideal mass distributions. In section 4 we evaluate the asphericity diagnostic for the SPARC galaxy rotation curves and show how the asphericity diagnostic is related to our previously developed HIDM model. The diagnostic is defined independently of any specific mass model.

## 2 Spherical inequalities

We derive spherical inequalities that can be violated when the rotation curve admits some asphericities. These inequalities are only based on the rotation curve v(r) and are model-independent. This makes them the perfect tool for asphericity detection in well measured rotation curves. However not all asphericities violate the inequality. Thus, if the inequality is violated (at an observationally robust level), asphericity of the DM halo is rigorously established, but the halo can be aspherical without violating the inequality.

**Continuous.** Consider a spherical mass distribution:  $v = \sqrt{\frac{GM}{r}}$  where M is the total mass inside the sphere of radius r. Then,  $\frac{dv}{dr} = \frac{\sqrt{G}}{2} \left( \frac{1}{r} \frac{dM}{dr} - \frac{M}{r^2} \right) \sqrt{\frac{r}{M}}$ , so

$$\frac{dv}{dr} = \frac{1}{2} \sqrt{\frac{G}{rM}} \frac{dM}{dr} - \frac{v}{2r}.$$
 (2.1)

Hence, since  $\frac{dM}{dr} \geq 0$ , we have the inequality

$$\Delta(r) \equiv 1 + \frac{v}{2r} \left(\frac{dv}{dr}\right)^{-1} \ge 0$$
, i.e., (2.2)

$$=1+\frac{d\ln r}{d\ln v}\ge 0\tag{2.3}$$

at all radii for any spherical mass distribution. Note  $\Delta < 0$  implies that the mass distribution is non-spherical but the existence of a non-spherical mass distribution does not imply  $\Delta < 0$ . For example, the Mestel disk [8, 9] is a disk distribution that has the same rotation curve as a point mass and therefore does not violate the spherical inequality.

**Discrete.** It is usefully to write the spherical inequality for discrete measurements since observations are at a discrete set of radii. Let i and j be 2 data points of a rotation curve with  $r_j > r_i$ . Then we have  $M_i \leq M_j$  where  $M_{i,j}$  is the total mass inside the sphere of radius  $r_{i,j}$ . Assume that the mass distribution is spherical:  $M_{i,j} = v_{i,j}^2 r_{i,j}/G$ . This leads to the inequality  $v_i^2 r_i \leq v_j^2 r_j$  and

$$\Delta_{ij} \equiv 1 - \frac{v_i}{v_j} \sqrt{\frac{r_i}{r_j}} \ge 0 \tag{2.4}$$

Mass model	Radial density	Comments
Exponential disk	$\Sigma(r) = \Sigma_0 e^{-r/r_0}$	detectable sphericity violation
Pseudo isothemal halo	$\rho(r) = \frac{\rho_0}{(1+r/r_0)^2}$	spherical
Oblate spheroid (Hubble profile) [9]	$\rho(m^2) = \rho_0 \left( 1 + \left( \frac{m}{r_0} \right)^2 \right)^{-3/2}$ with $m^2 = R^2 + \frac{z^2}{1 - e^2}$	e=1: flat, $e=0$ : spherical; no detectable sphericity violation
Einasto halo [10]	$\rho(r) = \rho_0 \exp\left(-\frac{2}{\alpha} \left(\frac{r}{r_0}\right)^{\alpha} - 1\right)$	spherical
Exponential disk + piso halo	$\rho(r,z) = \rho_{\text{piso}}(r) + \delta(z)\Sigma_{\text{exp}}(r)$	superposition of a disk and a halo
Annulus	$\Sigma(r) = \Sigma_0 \operatorname{rect}\left(\frac{r-r_0}{d}\right)$ with $\operatorname{rect}(r) = \begin{cases} 1 &  x  \leq \frac{1}{2} \\ 0 & \text{otherwise} \end{cases}$	produces a negative inner rotation curve

**Table 1.** Mass distribution examples. r is the radial (spherical) coordinate, R is the radial distance in cylindrical coordinates and z is the vertical distance.

for any spherical mass distribution. As phericity diagnostic  $\Delta$  can be used to detect as phericity: negative  $\Delta_{ij}$  implies that there exists some non-sperical structure such as a disk or a ring. Let  $\delta v$  be the error on velocity v. Then, the error on  $\Delta_{ij}$  is

$$\delta \Delta_{ij} = \sqrt{\frac{1}{v_j^2} \frac{r_i}{r_j} (\delta v_i)^2 + \frac{v_i^2}{v_j^4} \frac{r_i}{r_j} (\delta v_j)^2}.$$
 (2.5)

#### 3 Examples

In figures 1 and 2 we show the asphericity diagnostic  $\Delta$  for several different mass models: exponential disk, pseudo-isothermal halo, Hubble oblate spheroid, Einasto halo and a superposition of an exponential disk with the pseudo-isothermal (piso) halo (table 1). The exponential disk violates significantly the spherical inequality. The Hubble oblate spheroid is an example of a non-spherical distribution that doesn't violate the spherical inequality. When a halo is added to an exponential disk, if the halo is massive enough, the asphericity becomes undetectable. We illustrate this phenomena with a piso halo. If the exponential disk has the same scale radius  $r_0$  as the piso halo, the asphericity is detectable iff.  $c = \frac{\Sigma_0}{\rho_0 r_0} > 52.55$ .

# 4 Asphericity of the DM distribution in the SPARC galaxies

In this section, we compute  $\Delta_{ij}$  (2.4) for the DM contribution of the SPARC galaxies in order to seek unambigiously non-spherical DM structures. The contribution of the DM to

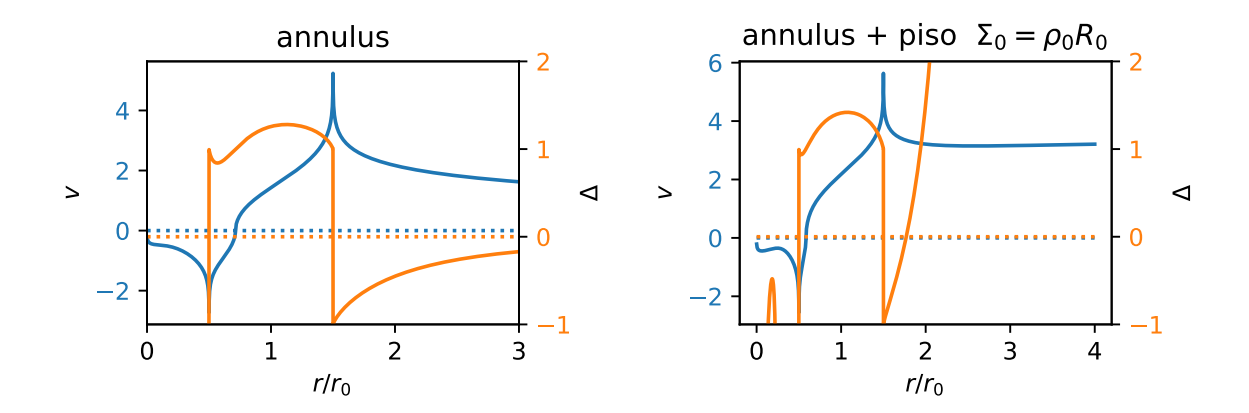


Figure 1. Left: blue: rotation curve of an annulus of inner radius  $r_0/2$  and outer radius  $3r_0/2$ . Orange: corresponding asphericity diagnostic  $\Delta$ . The inner negative rotation curve means that a test particle is pulled outward. This phenomena occurs in gas contributions to particular SPARC rotation curves when there are gas over-densities at a certain radius. Right: rotation curve and asphericity diagnostic for the superposition of a piso halo and an annulus with the same scale radius  $r_0$ , width  $d = r_0$  and  $\Sigma_0 = \rho_0 r_0$ .

the rotation curve is

$$v_{\rm DM}^2 = v_{\rm obs}^2 - \Upsilon_{\rm disk} v_{\rm disk}^2 - \Upsilon_{\rm bulge} v_{\rm bulge}^2 - v_{\rm gas}^2$$

$$\tag{4.1}$$

where  $v_{\rm obs}$  is the observed circular velocity,  $v_{\rm disk}$  and  $v_{\rm bulge}$  are the contributions of the stars to the observed velocity assuming a stellar mass-to-light ratio of  $1M_{\odot}/L_{\odot}$  and  $v_{\rm gas}$  is the contribution of the gas.  $\Upsilon_{\rm disk}$  and  $\Upsilon_{\rm bulge}$  are the stellar disk and bulge mass to light ratios. Note that  $v_i$  is not the velocity of the *i*th component. It is the contribution of the *i*th component to the total circular velocity and is derived by computing the gravitational potential of the *i*th component from the mass densities. The total gravitational potential is the sum of the contributions of each mass component and  $v_{\rm obs}^2 = \sum_i v_i^2$ . The main unknown is  $\Upsilon$ . In this work,  $\Upsilon$  is estimated by individually fitting each rotation curve with an Einasto halo [10]. We use the Einasto model because it can reproduce a great diversity of spherical halo shapes and has been show to fit the SPARC data particularly well [6, 11]. In order to obtain a realistic mean mass to light ratio around 0.5 as suggested by stellar population synthesis [12–14], the following term is added to the  $\chi^2$  when fitting, as in [6]:

$$\chi_{\Upsilon}^2 = \left(\frac{\Upsilon_{*,i} - \overline{\Upsilon}_*}{\sigma_{\Upsilon_*}}\right)^2 \tag{4.2}$$

where  $\overline{\Upsilon}_* = 0.5$  is the assumed mean mass to light ratio and  $\sigma_{\Upsilon_*}$  is the standard deviation of  $\overline{\Upsilon}_*$  values in an ensemble of galaxies, estimated to be  $\sigma_{\Upsilon_*} = 0.125; \Upsilon_{*,i} = \Upsilon_{\mathrm{disk},i}$  is the disk stellar mass to light ratio of the *i*th galaxy and  $\Upsilon_{\mathrm{bulge},i} = 1.4\Upsilon_{*,i}$  is the ratio for the bulge; see [6] for more information about these choices. The Einasto fits have 4 free parameters: 3 halo parameters and the stellar mass to light ratio.

<sup>&</sup>lt;sup>1</sup>In equation (4.2),  $\sigma_{\Upsilon_*}$  is a global parameter that represents the variance in the true stellar mass to light ratio of the ensemble of galaxies. Recall that each galaxy's stellar mass to light ratio is determined by fitting a Einasto halo to the rotation curve so  $\sigma_{\Upsilon_*}$  is not the error on  $\Upsilon_*$  for each individual fits. Since this error is not straightforward to estimate and the overall asphericity diagnostic significance is not sensitive to  $\overline{\Upsilon}_*$ , we do not include this error in the estimate of the error on  $\Delta_{ij}$  that is then fully determined by the error on the rotation curve measurements (equation (2.5)).

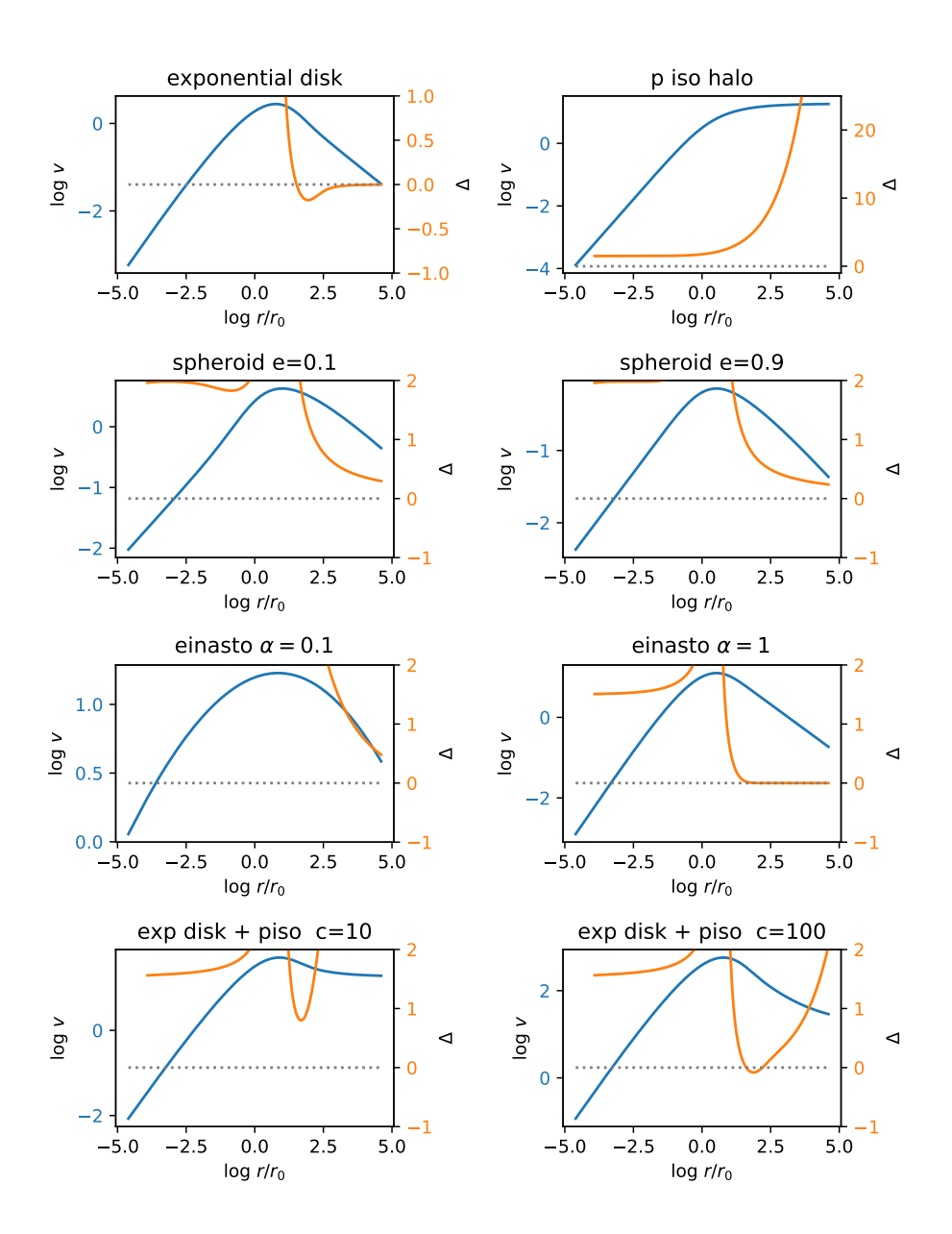


Figure 2. Rotation curve and asphericity diagnostic for various mass distributions; blue: rotation curve, Orange: asphericity diagnostic  $\Delta$ . Sphericity is violated when  $\Delta < 0$  and the slope of the log-log rotation curve is less than 1 (eq. (2.3)). The second row left plot corresponds to an almost spherical spheroid while the right one corresponds to an almost flat spheroid. Note that even thought these spheroids are not spherically symmetric mass distributions,  $\Delta$  is positive and this quantity cannot be used to detect asphericity in this case. The two bottom models are a superposition of a pseudo-isothermal halo and an exponential disk with the same scale radius  $R_0$  and  $c = \frac{\Sigma_0}{\rho_0 R_0}$ . The asphericity is detectable via a negative  $\Delta$  iff. c > 52.55.

For each galaxy we compute a set of  $\Delta_{ij}$  where i, j are neighbor data points, then we combine the significances of these values in order to determine the significance that a given galaxy violates sphericity. The error on the DM contribution that is used in eq. (2.5) is

$$\delta v_{\rm DM} = \frac{v_{\rm obs}}{v_{\rm DM}} \delta v_{\rm obs}. \tag{4.3}$$

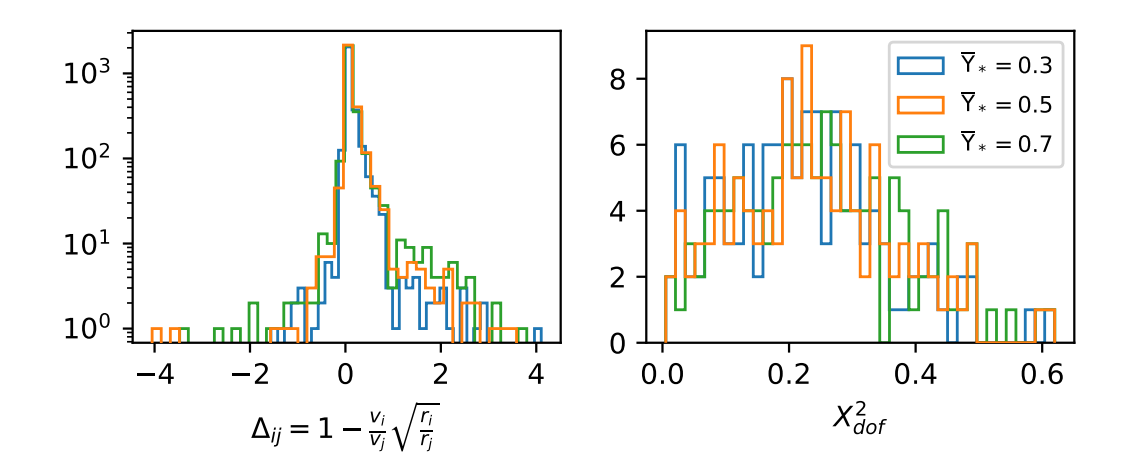


Figure 3. Left: distribution of the  $\Delta_{ij}(v_{\rm DM})$  values for all i,j neighbors datapoints of the SPARC rotation curves. Right: distribution of  $\chi^2_{\rm dof}$  per galaxy for three values of mean stellar mass to light ratios, showing that the choice of mean  $\Upsilon^*$  does not significantly change the conclusions. The individual mass to light ratios are determined using Einasto fits.

The p-value that one data-point k does not violate sphericity (i.e that  $\Delta$  is positive) is the Gaussian integral

$$p_k = \frac{1}{\sigma_k \sqrt{2\pi}} \int_0^\infty \exp\left(-\frac{1}{2} \left(\frac{x - \Delta_k}{\sigma_k}\right)^2\right) dx \tag{4.4}$$

$$= \frac{1}{2} \left( 1 + \operatorname{Erf}\left(\frac{\Delta_k}{\sqrt{2}\sigma_k}\right) \right) \tag{4.5}$$

with  $\Delta_k = \Delta_{k,k+1}$  and  $\sigma_k = \delta \Delta_k$  (defined in eq. (2.5)). Note that  $p_k \sim 0$  means that datapoint k shows significant sphericity violation while  $p_k \sim 1$  means that data-point k does not show sphericity violation. Using Fisher's method for each galaxy, define

$$\chi^2 = -2\sum_{k=1}^n \ln(p_k). \tag{4.6}$$

If the  $p_k$  are independent random variables drawn from the uniform distribution [0,1], then  $\chi^2$  follows a  $\chi^2$  distribution with 2n degrees of freedom. Hence we define  $\chi^2_{\rm dof} = \frac{1}{2n}\chi^2$ . Now we see that  $\chi^2_{\rm dof} \sim 1$  implies that there is no preference for asphericity nor sphericity, while  $\chi^2_{\rm dof} > 1$  implies that the  $p_k$  are biased toward 0 and that there is a significant preference for asphericity. We find that  $\chi^2_{\rm dof} < 1$  for every galaxy in the SPARC dataset and sphericity is not manifestly violated within the measurement uncertainties; this is shown in figure 3. In figures 5 and 6, we show a sample of 12 galaxies from SPARC that exhibit at least one significantly negative  $\Delta$  value.

Given the error provided by SPARC, these negative  $\Delta$  values are not sufficient to give evidence for asphericity. More precise measurements of these particular galaxies' rotation curves are needed in order to determine whether any of these galaxies may contain non-spherical DM structures of the types detectable through a region of negative  $\Delta$ .

Given the present large error bars on the  $\Delta$  values from SPARC, the statistical indicator derived above is not very useful for identifying promising candidate galaxies which may have

DM structure detectable through a negative  $\Delta$ . As an alternate approach, we use our fit to the SPARC rotation curves for the hadronically interacting dark matter (HIDM) model developed in [6], and calculate  $\Delta(r)$  for the model DM distribution. This model includes a piso halo and a DM disk that scales the interaction rate per unit volume between the gas particles in the gas disk and DM particles in the DM halo. The radial density of the DM disk is

$$\Sigma_{\rm DM}(r) = \zeta \,\rho_{\rm halo}(r) \,v_{\rm obs}(r) \,\Sigma_{\rm gas}(r) \tag{4.7}$$

where  $\zeta$  is a galaxy-dependent free parameter. This leads to a model where the total observed velocity is

$$v_{\text{HIDM}}^2 = \Upsilon_{\text{disk}} v_{\text{disk}}^2 + \Upsilon_{\text{bulge}} v_{\text{bulge}}^2 + v_{\text{gas}}^2 + v_{\text{DMdisk}}^2 + v_{\text{pIso}}^2$$
(4.8)

where  $v_{\text{pIso}} = 4\pi G \rho_0 R_c^2 \left(1 - \frac{R_c}{r} \tan^{-1} \left(\frac{r}{R_c}\right)\right)$  with free parameters  $R_c$  and  $\rho_0$ ; the contribution of the DM disk  $v_{\text{DMdisk}}$  is derived from equation (4.7). The model has a total of 4 free parameters  $R_c$ ,  $\rho_0$ ,  $\zeta$  and  $\Upsilon_*$  per galaxy. The fitting procedure is explained in more detail in [6].

These fits allows us to select 4 galaxies that have particularly massive DM disks (figure 4). The two galaxies in the upper row should have an in-principle-detectable-negative asphericity diagnostic stemming from their non-spherical DM component, according to our HIDM model fit. (While the fit to UGC06614 yields a small negative value of  $\Delta$  at large radius, it may be undetectably small.) This means that if the model holds and if the uncertainty on the measurements were low enough, it would be possible to detect non-spherical structures by measuring the asphericity diagnostic for their rotation curves. Fit results for a selection of other galaxies are summarized in table 2, showing that a number of other galaxies are also good candidates to display a negative  $\Delta$ .

#### 5 Conclusion

We have introduced an asphericity diagnostic  $\Delta$ , whose positivity is a necessary condition for a spherically symmetric distribution. In section 3 we showed that the asphericity of some mass distributions such as exponential disks and rings can be detected using this tool, via a negative value of asphericity parameter  $\Delta$ .

In section 4, the diagnostic is tested on real rotation curves in the SPARC dataset in order to look for non-spherical dark matter structures. Overall, there is no strong evidence for non-spherical DM structures in the studied dataset given the precision of the measurements. However, with more precise measurements this tool could be a useful diagnostic of non-spherical DM structures that could emerge from baryon interactions. Given that the distribution of significance  $\chi^2_{\rm dof}$  of the asphericity diagnostic peaks around 0.2 (figure 3 right), the exact same measurements with an error  $\sqrt{5}$  smaller could show significant asphericity. Note that this is only a lower bound on the required increase in needed precision assuming identical measurement values.

The five SPARC galaxies with the highest dark matter asphericity significance are NGC5005, UGCA444, UGC11914, NGC7793 and UGC05253, with  $\chi^2_{\rm dof} = 0.48, 0.49, 0.61, 0.59, 0.48$  respectively;  $\chi^2_{\rm dof}$  is defined (see section 4) such that  $\chi^2_{\rm dof} \geq 1$  would be a robust indicator of asphericity. The five galaxies with the highest percentage of negative  $\Delta$  values are NGC2683, F563-1, UGC11914, NGC6015, NGC7793 with 30, 18, 21, 20, 33% of negative values respectively. Currently, the error bars on the rotation curves are too high for these to be significant evidence of non-spherically symmetric dark matter. Moreover based on the

name	$\chi^2_{ m dof}$	name	$\Delta$	name	min $\Delta$	name	$\Delta$	name	min $\Delta$
							HIDM		HIDM
UGC11914	0.620	NGC7793	0.333	NGC7793	-54.151	NGC7793	0.333	NGC4088	-14.914
NGC7793	0.598	NGC2683	0.300	$\mathrm{UGC02885}$	-4.064	NGC3521	0.325	NGC2915	-4.485
UGCA444	0.494	UGC11914	0.219	UGC11557	-3.589	NGC2683	0.300	NGC6195	-3.999
NGC5005	0.484	NGC6015	0.209	NGC5585	-1.517	NGC2955	0.261	${\rm UGC05253}$	-2.994
$\mathrm{UGC05253}$	0.482	F563-1	0.188	NGC4088	-1.338	NGC6195	0.227	NGC3521	-2.165
ESO563-G021	0.467	NGC6195	0.182	NGC6195	-1.043	UGC11914	0.219	NGC0891	-2.112
NGC2915	0.461	IC2574	0.182	ESO563-G021	-0.885	F563-1	0.188	$\Omega$ CC06787	-0.964
NGC2683	0.454	UGC11557	0.182	$\mathrm{UGC05253}$	-0.788	IC2574	0.182	UGC02885	-0.952
NGC3521	0.449	NGC3726	0.182	NGC6946	-0.704	UGC11557	0.182	NGC5585	-0.896
NGC6946	0.433	NGC6946	0.175	UGC11914	-0.584	NGC2915	0.172	NGC7793	-0.883
NGC4013	0.426	UGC11455	0.143	$\mathrm{UGC03546}$	-0.560	NGC4013	0.171	NGC7331	-0.788
NGC4559	0.415	NGC5033	0.143	$\mathrm{UGC02953}$	-0.485	NGC2998	0.167	$\Omega$ CC08699	-0.707
$\mathrm{UGC02953}$	0.409	UGC05253	0.139	F583-1	-0.321	NGC5033	0.143	UGC11914	-0.585
NGC6195	0.406	NGC2915	0.138	$\Omega$ CC08699	-0.303	UGC02916	0.143	$\mathrm{UGC02953}$	-0.520
$\mathrm{UGC}12506$	0.405	UGC03546	0.138	NGC0289	-0.302	NGC6946	0.140	$\mathrm{UGC03546}$	-0.473
NGC0289	0.391	UGC12506	0.133	NGC4157	-0.211	NGC6015	0.140	NGC2955	-0.421
F563-1	0.384	NGC2955	0.130	NGC4013	-0.106	UGC12506	0.133	UGC11557	-0.390
NGC2976	0.376	NGC2976	0.115	NGC3726	-0.103	UGC02953	0.132	UGC02916	-0.345
UGC11557	0.374	NGC4013	0.114	UGC11455	-0.083	NGC2403	0.125	F583-1	-0.327
F583-1	0.369	UGC02953	0.114	${ m UGC}09037$	-0.080	UGC05253	0.125	NGC2998	-0.298

significant galaxies are displayed.  $\chi^2_{\rm dof}$  is the asphericity diagnostic defined in equation (4.6). 'neg  $\Delta$ ' is the fraction of negative  $\Delta$  values in the rotation curve. HIDM indicates that the indicator is calculated based on a HIDM model fit to the rotation curve as explained in the end of section 4. Note that the full dataset has 121 galaxies. Table 2. List of galaxies with significant non-sperical DM component. Each column is sorted according to one indicator and only the 20 most

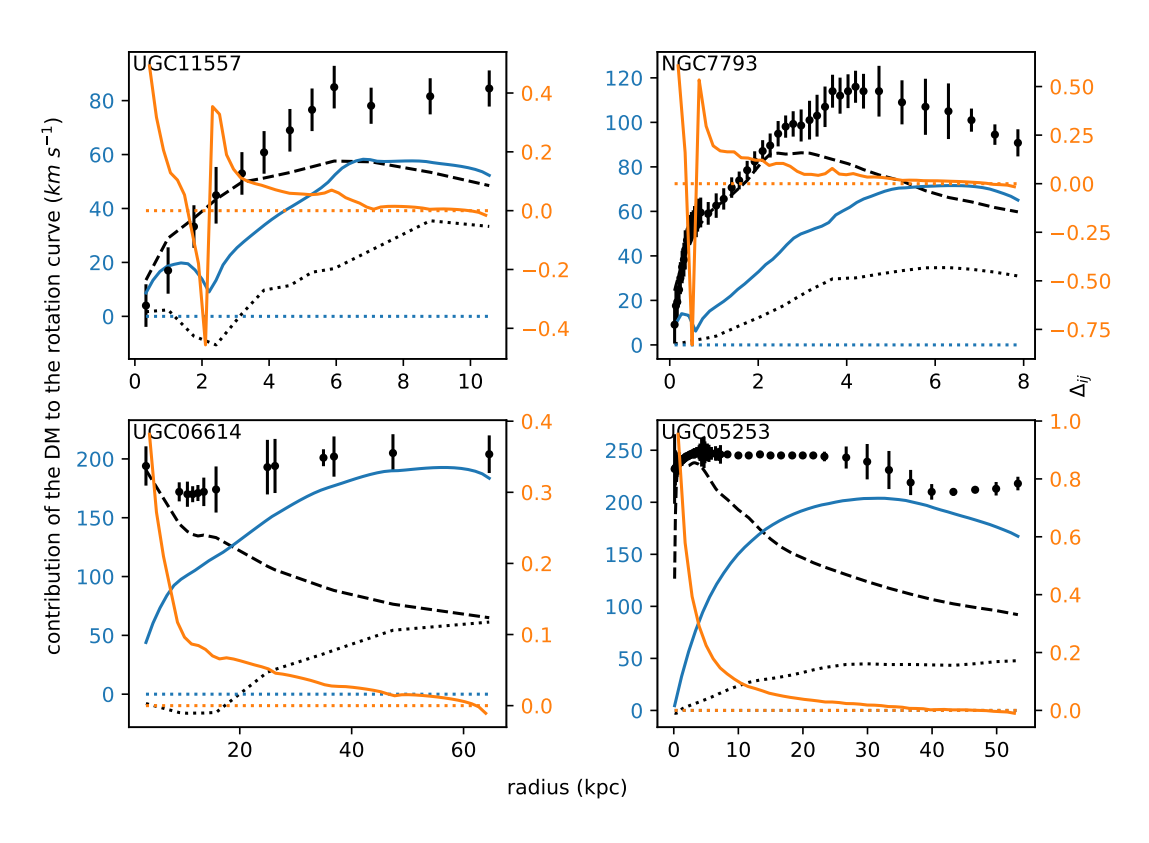


Figure 4. Sample of 4 galaxies that have a particularly massive DM disk in the HIDM-IS model. Black markers: observed rotation curve; dashes: stellar contribution displayed with the optimal  $\Upsilon_*$ ; dots: gas contribution. (Since stars form from gas, it is natural that in UGC11557 one sees similar structure in stars as in gas.) The blue line is the model DM contribution that is the superposition of a disk and a halo. The orange line is the asphericity diagnostic derived from this DM rotation curve. The presence of a non-spherical DM distribution can in principle be detectable in the top two, using the asymmetry diagnostic introduced here, but the signature would not be strong enough in the lower pair.

HIDM fit of [6] the DM distribution in these galaxies — in spite of not being spherical — would not be expected to be manifestly asymmetric in the manner needed for the asphericity diagnostic to reveal it. More results for individual galaxies are summarized in table 2.

Using the HIDM model fit from [6], we identified four galaxies that are compatible with a particularly heavy dark mater disk built up through DM accretion in the baryonic disk: UGC11557, NGC7793, UGC06614 and UGC05253. These are displayed in figure 4 where it can be seen that NGC7793 and UGC05253 may be good candidates for future detection of small-scale structure in the dark matter distribution using the asphericity diagnostic, if measurement accuracy can be sufficiently improved.

Independently of the HIDM model of [6], galaxies displaying a strong variation in the radial distribution of gas are the best candidates for having  $\Delta < 0$ , if any galaxies do. A DM ring would be a smoking gun for HIDM interactions, and would be strongest in galaxies with the strongest gas rings. The measurement error bars in figure 4 include rough systematic errors assigned by the SPARC collaboration which can be reduced by more precise modeling

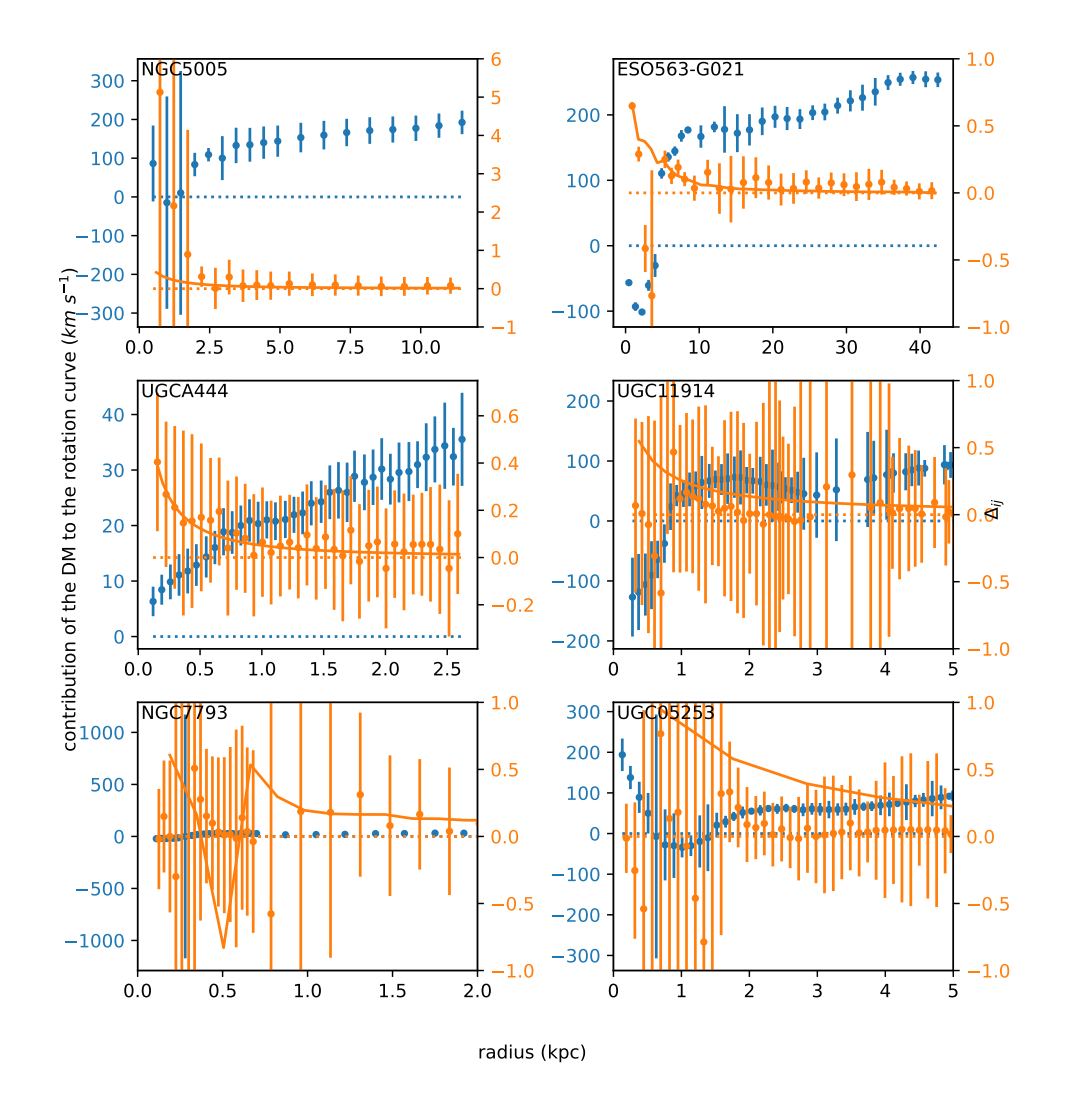
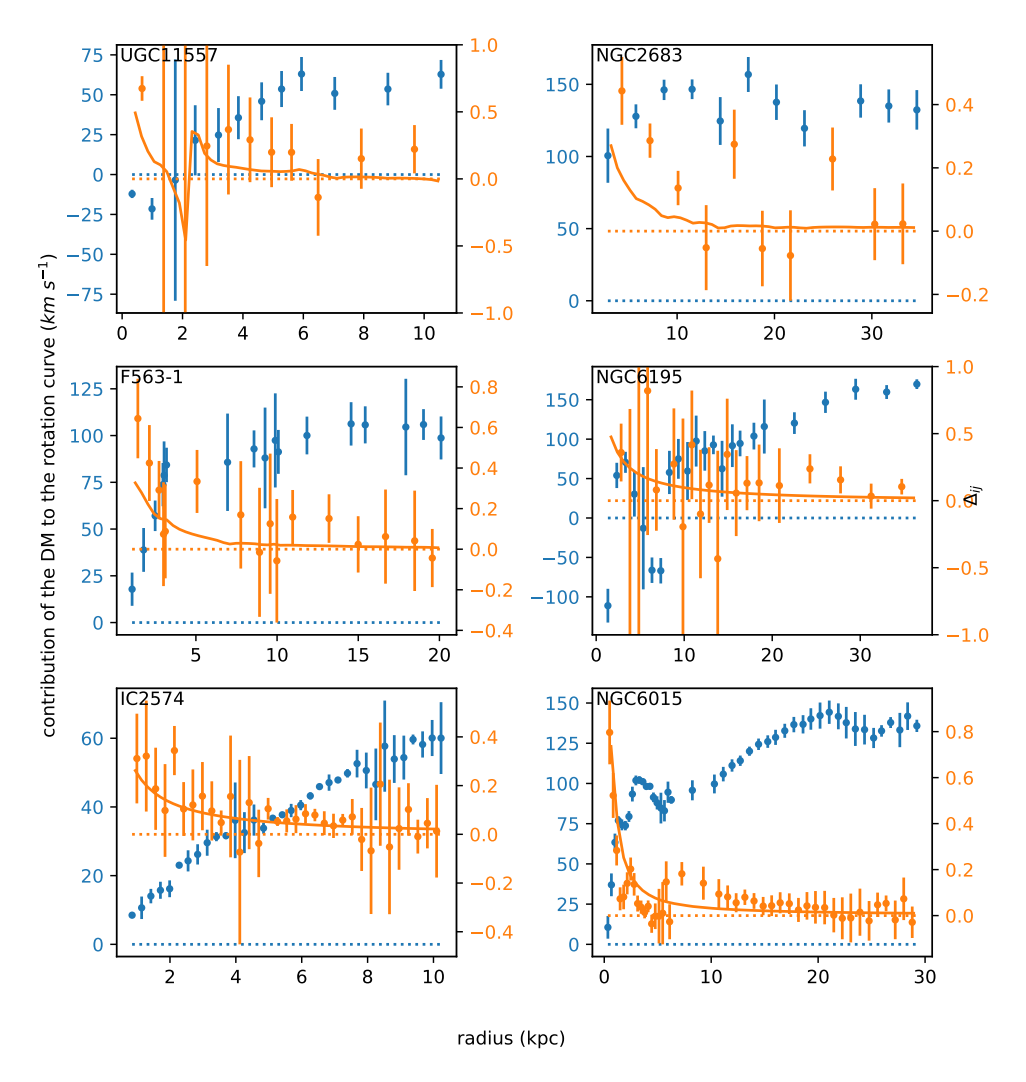


Figure 5. Sample of 6 galaxies with the highest likelihood of showing a non-trivial asphericity diagnostic with better data, based on their current  $\chi^2_{\text{dof}}$  values (eq. (4.6)) based on the SPARC measurements. Blue markers: contribution of the DM to the rotation curve. Orange markers: discrete asphericity diagnostic  $\Delta_{ij}$ . Orange solid line: asphericity diagnostic predicted by the HIDM model fit. A significantly negative  $\Delta_{ij}$  would show the presence of DM structures like rings, or disks that make the rotation curve drop faster than a spherical distribution. The error is computed assuming that there is no error on the mass to light ratio determination using equation (2.5). Different mass to light ratios imply different DM contributions and therefore different  $\Delta_{ij}$ , so in a future attempt to detect asphericity, the mass-to-light ratio should be determined by stellar population synthesis modeling for each galaxy to be studied.

of the radial velocity data, suggesting that the required reduction of errors in  $\Delta$  can be within reach.

In sum, to most effectively investigate whether there is a non-trivial small-scale structure in DM, as a result of DM collecting with gas, the following observational procedure is suggested:

1. Identify galaxies for which good rotation curves can be obtained (viewing angle neither too edge-on or flat-on).



**Figure 6**. Sample of 6 galaxies with the highest percentage of negative  $\Delta$  values. Same legend as figure 5.

- 2. Identify a subset of galaxies with strong radial variations in gas or gas+stars, especially ring-like structures.
- 3. Make accurate measurements of the circular velocity as well as the mass distribution of gas and stars in the radial region enclosing the gas structure, with high radial resolution. It is crucial to measure all of these accurately, to accurately find the DM contribution. It is not necessary to improve the measurements at large radii far beyond the gas, which is fortunate since tracing the rotation curve at large radius can be difficult.
- 4. Perform detailed stellar-population modeling of these individual galaxies, in order to accurately assign the correct stellar mass-to-light ratio, which may change as a function of radius.

Using this data, the DM contribution to the rotation curves of the selected galaxies can be determined, so the local asphericity diagnostic  $\Delta$  introduced here can be measured. Finding that  $\Delta < 0$  with sufficiently small statistical and systematic error bars, even at one radial

position, would provide unambiguous proof that DM has a spherical structure. (Of course, observing it at a sequence of radii and in multiple galaxies would be needed to become convinced.) The last two columns of table 2 can be helpful in selecting promising galaxies for detecting a negative  $\Delta$ , based on the HIDM modeling of [6]. Perhaps the most favorable three in the SPARC dataset, in terms of a strong signal covering a significant radial region according to the HIDM fit, would be NGC2915, 6195 and 3521, while independently of the model, NGC7793 and UGC1155 are good candidates.

#### Acknowledgments

The research of G.R.F. is supported in part by NSF-PHY-2013199 and by the Simons Foundation.

## References

- [1] V.C. Rubin, N. Thonnard and W.K.N. Ford Jr., Rotational properties of 21 SC galaxies with a large range of luminosities and radii, from NGC 4605 (R = 4 kpc) to UGC 2885 (R = 122 kpc), Astrophys. J. 238 (1980) 471 [INSPIRE].
- [2] J. Fan, A. Katz, L. Randall and M. Reece, *Double-disk dark matter*, *Phys. Dark Universe* **2** (2013) 139.
- [3] K. Schutz, T. Lin, B.R. Safdi and C.-L. Wu, Constraining a Thin Dark Matter Disk with Gaia, Phys. Rev. Lett. 121 (2018) 081101 [arXiv:1711.03103] [INSPIRE].
- [4] J. Buch, S.C.J. Leung and J. Fan, Using Gaia DR2 to Constrain Local Dark Matter Density and Thin Dark Disk, JCAP 04 (2019) 026 [arXiv:1808.05603] [INSPIRE].
- [5] M. McCullough and L. Randall, Exothermic Double-Disk Dark Matter, JCAP 10 (2013) 058
   [arXiv:1307.4095] [INSPIRE].
- [6] N. Loizeau and G.R. Farrar, Galaxy Rotation Curves Disfavor Traditional and Self-interacting Dark Matter Halos, Preferring a Disk Component or Einasto Function, Astrophys. J. Lett. 920 (2021) L10 [arXiv:2105.00119] [INSPIRE].
- [7] F. Lelli, S.S. McGaugh and J.M. Schombert, SPARC: Mass Models for 175 Disk Galaxies with Spitzer Photometry and Accurate Rotation Curves, Astron. J. 152 (2016) 157 [arXiv:1606.09251] [INSPIRE].
- [8] L. Mestel, On the galactic law of rotation, Mon. Not. Roy. Astron. Soc. 126 (1963) 553.
- [9] J. Binney and S. Tremaine, Galactic dynamics, Princeton University Press, Princeton NJ U.S.A. (1987).
- [10] J. Einasto, On the Construction of a Composite Model for the Galaxy and on the Determination of the System of Galactic Parameters, Trudy Astrofiz. Inst. Alma-Ata 5 (1965) 87.
- [11] P. Li, F. Lelli, S. McGaugh and J. Schombert, A comprehensive catalog of dark matter halo models for SPARC galaxies, Astrophys. J. Suppl. Ser. 247 (2020) 31.
- [12] J. Schombert and S. McGaugh, Stellar populations and the star formation histories of LSB galaxies. Part III. Stellar population models, Publ. Astron. Soc. Austral. 31 (2014) e036.
- [13] S.S. McGaugh and J.M. Schombert, Color-Mass-to-light-ratio Relations for Disk Galaxies, Astron. J. 148 (2014) 77.
- [14] S.E. Meidt et al., Reconstructing the stellar mass distributions of galaxies using S<sup>4</sup>G IRAC 3.6 and 4.5 μm images. Part II. The conversion from light to mass, Astrophys. J. 788 (2014) 144 [arXiv:1402.5210] [INSPIRE].